

Exploring the 3D quark and gluon structure of the proton: Electron scattering with present and future facilities*

H. Abramowicz,¹ A. Afanasev,² H. Avakian,³ M. Burkardt,⁴ V. Burkert,³ A. Camsonne,³ A. Deshpande,^{5, 6}
 F. Ellinghaus,⁷ L. Elouadrhiri,³ R. Ent,³ M. Garçon,⁸ G. Gavalian,⁹ M. Guidal,¹⁰ V. Guzey,¹¹
 C. E. Hyde,^{9, 12} X.-D. Ji,¹³ A. Levy,¹ S. Liuti,¹⁴ W. Melnitchouk,³ R. G. Milner,¹⁵ Ch. Montag,¹⁶
 D. Müller,¹⁷ C. Muñoz Camacho,¹⁸ R. Niyazov,³ B. Pasquini,¹⁹ S. Procureur,⁸ A. Radyushkin,^{3, 9} J. Roche,²⁰
 F. Sabatié,⁸ A. Sandacz,²¹ A. Schäfer,¹⁷ M. Strikman,²² M. Vanderhaeghen,^{3, 23} E. Voutier,²⁴ and C. Weiss³

¹*Tel Aviv University, Tel Aviv 61390, Israel*

²*Hampton University, Hampton, Virginia 23668, USA*

³*Jefferson Lab, Newport News, Virginia 23606, USA*

⁴*Department of Physics, New Mexico State University, Las Cruces, New Mexico 88003, USA*

⁵*Department of Physics and Astronomy, Stony Brook University, SUNY, Stony Brook, New York 11794, USA*

⁶*RIKEN BNL Research Center, Brookhaven National Lab, Upton, New York 11973, USA*

⁷*Department of Physics, University of Colorado, Boulder, Colorado 80309, USA*

⁸*DAPNIA/SPhN, CEA-Saclay, France*

⁹*Old Dominion University, Norfolk, Virginia 23529, USA*

¹⁰*Institut de Physique Nucleaire Orsay, Orsay, France*

¹¹*Institut für Theoretische Physik II, Ruhr-Universität Bochum, 44780 Bochum, Germany*

¹²*Laboratoire de Physique Corpusculaire, Université Blaise Pascal, 63177 Aubièrre, France*

¹³*Department of Physics, University of Maryland, College Park, Maryland 20742, USA*

¹⁴*University of Virginia, Charlottesville, Virginia 22904, USA*

¹⁵*Massachusetts Institute of Technology, Cambridge, Massachusetts 02139, USA*

¹⁶*Brookhaven National Lab, Upton, New York 11973, USA*

¹⁷*Institut für Theoretische Physik, Universität Regensburg, 93040 Regensburg, Germany*

¹⁸*Los Alamos National Lab, Los Alamos, New Mexico 87545, USA*

¹⁹*Dipartimento di Fisica Nucleare e Teorica, Università degli Studi di Pavia and INFN, Sezione di Pavia, Pavia, Italy*

²⁰*Ohio University, Athens, Ohio 45701, USA*

²¹*Soltan Institute for Nuclear Studies, Warsaw, Poland*

²²*Pennsylvania State University, University Park, Pennsylvania 16802, USA*

²³*Department of Physics, College of William and Mary, Williamsburg, Virginia 23187, USA*

²⁴*Laboratoire de Physique Subatomique et de Cosmologie,
Université Joseph Fourier, 38026 Grenoble, France*

Understanding the structure of the nucleon in terms of the quark and gluon degrees of freedom of QCD is one of the key objectives of nuclear physics. During the last 10 years a comprehensive framework for describing the quark and gluon structure of the nucleon has been developed, based on the concept of Generalized Parton Distributions (GPDs). GPDs unify the momentum-space parton densities measured in inclusive deep-inelastic electron scattering with the spatial densities (form factors) measured in elastic scattering. They describe correlations between the momentum and spatial distributions of quarks, which are revealed in exclusive processes in electron scattering at large momentum transfer (deeply virtual Compton scattering, meson production). GPDs are the basis for novel representations of the nucleon as an extended object in space (2-dimensional tomographic images, 3-dimensional Wigner phase space distributions), and provide access to fundamental static properties such as the quark orbital angular momentum. In this White Paper we summarize the scientific motivation for nucleon structure studies based on GPDs, and outline what measurements with present and future facilities can contribute to our knowledge of these functions. We specifically focus on the GPD program planned with the 12 GeV Upgrade of Jefferson Lab, and on GPD studies with a future electron-ion collider (EIC).

* White Paper prepared for the discussion of the National Science Advisory Committee's Long-Range Plan (2007). Drafted at the Workshop "Hard exclusive processes with JLab 12 GeV and a future EIC," University of Maryland, Oct. 29-30, 2006, organized jointly by the Institute of Nuclear Theory, Jefferson Lab, and Brookhaven National Lab. The individual contributions to the Workshop are available at <http://www.physics.umd.edu/tqhn/GPD.html>.

I. INTRODUCTION

Nucleons — protons and neutrons — are the basic building blocks of atomic nuclei. The mass stored in these particles makes up more than 99% of the mass of the visible Universe. The strong interactions between nucleons determine the properties of nuclei, which in turn defines the chemical elements and leads to the myriad of structures observed at the atomic and molecular level. They also govern the dynamics of nuclear reactions, which have shaped the evolution of the early Universe, fuel the Sun, and form the basis of all uses of nuclear energy. The interactions between nucleons, in turn, are an expression of their complex internal structure — a fact which makes the physics of strong interactions a uniquely challenging problem. Unraveling the internal structure of the nucleon is the key to understanding phenomena at the nuclear and astrophysical level. The importance of this problem can be likened to that of unraveling the DNA of organisms for the understanding of their biological functions.

Electron scattering has proved to be one of the most powerful experimental tools for exploring the internal structure of the nucleon. Historically, such experiments provided two crucial insights which revolutionized our understanding of strong interactions. First, elastic electron scattering (where the nucleon is left intact) established the extended nature of the nucleon (Hofstadter, Nobel Prize 1961). Such experiments measure the form factors, which describe the spatial distributions of electric charge and current inside the nucleon. Second, inelastic electron scattering at large energy and momentum transfers (where the nucleon disintegrates into hadrons) provided evidence for the existence of quasi-free, pointlike constituents at short distance scales, the quarks (Friedman, Kendall, and Taylor, Nobel Prize 1990). This eventually established Quantum Chromodynamics (QCD) as the fundamental theory of strong interactions, a quantum field theory exhibiting the celebrated property of asymptotic freedom — the vanishing of the interaction at short distances (Gross, Politzer, and Wilczek, Nobel Prize 2004). Later inelastic scattering experiments made detailed measurements of the momentum distribution of quarks in the nucleon along the reaction axis, the parton distributions.

The structures probed in elastic and inelastic electron scattering — form factors and parton distributions — have traditionally been discussed as separate concepts, with no apparent relation between them. Only recently was it realized that in fact they represent special cases of a more general, much more powerful, way to characterize the structure of the nucleon, the generalized parton distributions (GPDs). The GPDs are the Wigner quantum phase space distribution of quarks in the nucleon — functions describing the simultaneous distribution of particles with respect to both position and momentum in a quantum-mechanical system, representing the closest analog to a classical phase space density allowed by the uncertainty principle. In addition to the information about the spatial densities (form factors) and momentum densities (parton distributions), these functions reveal the correlation of the spatial and momentum distributions, *i.e.*, how the spatial shape of the nucleon changes when probing quarks and gluons of different wavelengths.

The concept of GPDs has in many ways revolutionized how scientists think about the structure of the nucleon. First, it has led to completely new methods of “spatial imaging” of the nucleon, either in the form of 2-dimensional tomographic images (analogous to Computer Tomography scans in medical imaging), or in the form of genuine 3-dimensional images (Wigner distributions). Second, GPDs allow us to quantify how the orbital motion of quarks in the nucleon contributes to the nucleon spin — a question of crucial importance for our understanding of the “mechanics” underlying nucleon structure. Third, the spatial view of the nucleon enabled by the GPDs provides us with new ways to test dynamical models of nucleon structure. Traditional phenomenological concepts of hadronic physics such as the nucleon’s quark core, the pion cloud, and the gluon field probed in high-energy scattering, can be rigorously formulated — and most naturally be understood — within this new representation.

The mapping of the nucleon GPDs, and a detailed understanding of the spatial quark and gluon structure of the nucleon, are widely recognized as one of the key objectives of nuclear physics of the next decade. It requires a comprehensive program, combining results of measurements of a variety of processes in electron-nucleon scattering with structural constraints obtained from theoretical studies, as well as with expected results from future lattice QCD simulations. Important basic information is provided by the extensive data on nucleon form factors and parton distributions collected in elastic and inelastic electron scattering experiments over the last 20 years. The crucial new information about the correlation of the spatial and momentum distributions — essential for nucleon imaging and the extraction of the quark orbital angular momentum — will come from measurements of exclusive processes at large momentum transfer, namely deeply-virtual Compton scattering (DVCS), $eN \rightarrow eN\gamma$, and meson production, $eN \rightarrow eNM$ (where $M = \pi, \rho, K, \phi, J/\psi$, etc.). Such measurements require a combination of high energy and high beam intensity, and are generally much more challenging than traditional inclusive scattering experiments. This ambitious program makes full use of recent advances in accelerator and detector technology; in fact, it already has

proved to be a major impetus for further developments in these fields. The basic feasibility of such measurements has been demonstrated in a number of exploratory studies. The theoretical analysis of these measurements relies on the idea of “factorization” of the amplitudes in a short–distance quark scattering process, calculable using well–tested methods of perturbative QCD, and long–distance matrix elements describing the distribution of quarks in the nucleon — the GPDs, which are to be extracted from the data.

This White Paper is an attempt to summarize what electron scattering experiments with present and future facilities can contribute to the program of exploring nucleon structure in terms of GPDs. We specifically focus on two facilities presently planned or under consideration in the U.S.: The 12 GeV Upgrade of Jefferson Lab (JLab), and a future Electron–Ion Collider (EIC). The paper is intended to provide information for the discussions of the National Science Advisory Committee’s Long–Range Plan by the scientific community, presently under way in the U.S.

The JLab 12 GeV Upgrade is a Department of Energy project which prepares for an increase of the energy of the CEBAF continuous–beam electron accelerator from 6 to 12 GeV, as well as upgrades of the detection equipment in the experimental halls. This setup will provide unprecedented capabilities for exploring nucleon structure in the valence quark region, and for meson spectroscopy in the few–GeV mass region. In particular, it will provide the unique combination of high beam intensity (luminosity), high energy, and advanced detection capabilities necessary to study low–rate processes such as DVCS and exclusive meson production. The study of the nucleon’s quark GPDs in the valence quark region is one of the key objectives of the Upgrade project [1]. An EIC is mentioned as one of the future high–priority projects in the last DOE 20–year plan. Such a machine would collide a high–energy electron beam with a proton or ion beam, reaching considerably higher center–of–mass energies and momentum transfers than fixed–target experiments. Realizing within this accelerator concept the high beam intensities and beam polarization necessary for detailed studies of nucleon structure represents a major technological challenge. Extensive studies by accelerator experts during the last years have resulted in specific designs, which differ in their emphasis on the realization of high energies and high luminosities [2, 3]. An EIC would support a rich physics program including studies of the nucleon’s gluon polarization, QCD in the regime of high gluon densities, and the effect of the nuclear medium on the nucleon’s quark and gluon distributions. In particular, it would provide a unique opportunity to probe the nucleon GPDs in exclusive processes at high energies, where gluons and “sea” quarks generated by QCD radiation are the dominant degrees of freedom.

The capabilities provided by the 12 GeV Upgrade of JLab and a future EIC are complementary, and combine to a comprehensive experimental program of exploring nucleon structure in terms of GPDs. A two–stage approach, where measurements with JLab at 12 GeV map the GPDs in the valence quark region (which can be done only in fixed–target experiments with the CEBAF high–intensity beam), and the EIC extends these studies to the gluon and sea quark GPDs (which can only be done in high–energy scattering with a collider) would be an ideal scenario for the long–term future of QCD–based nucleon structure studies, and enjoys the support of the vast majority of the nuclear physics community. The purpose of the present White Paper is to chart the course along this promising direction.

II. 3D QUARK/GLUON IMAGING OF THE NUCLEON WITH GPDs

GPDs, in basic terms, describe the structure of the nucleon probed in reactions in which a high–energy, short–distance probe interacts with a *single quark* in the nucleon. Mathematically, this is the quantum–mechanical amplitude for “taking out” a quark of the wave function of the fast–moving nucleon and “putting it back” with different momentum, thereby imparting a certain momentum transfer to the nucleon [4–6]. It depends on the fractions of the nucleon momentum carried by the quark before and after the process, usually denoted by $x - \xi$ and $x + \xi$ (where 2ξ is the fractional longitudinal momentum transfer to the nucleon), as well as on the transverse momentum transfer to the nucleon, Δ_{T} . In the special case of zero momentum transfer to the nucleon, $\xi = 0$ and $\Delta_{\text{T}} = 0$, this amplitude reduces to the usual parton density of quarks in the nucleon at momentum fraction x , as measured in inclusive deep–inelastic eN scattering (DIS). Similarly, in the case of non–zero transverse momentum transfer, $\Delta_{\text{T}} \neq 0$, the integral of the GPD over x reduces to the nucleon form factor at invariant momentum transfer $t = -\Delta_{\text{T}}^2$, as measured in elastic eN scattering. Thus, the GPDs combine the traditional concepts of parton density and elastic form factor within a single structure. The different possible spin polarizations of the nucleon and the quark and the presence of different quark flavors (u, d, s) lead to the appearance of various independent spin/ flavor components of the GPDs. Finally, the gluon GPDs are defined in complete analogy to the quarks. Together, these functions provide a comprehensive description of the quark and gluon structure of the nucleon (see Refs. [7–9] for reviews).

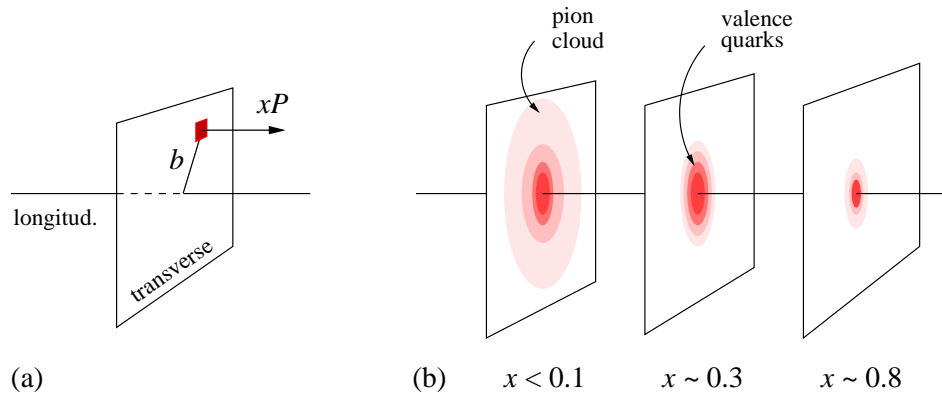


FIG. 1: Nucleon tomography: (a) The transverse Fourier transform of the GPD describes the distribution of quarks with longitudinal momentum fraction x with respect to transverse position, b [10]. (b) It produces a set of 2-dimensional “tomographic” image of the quark structure of the nucleon, which allows one to clearly identify the contributions from the valence quarks ($x \geq 0.3$, moderate b), the pion cloud ($x \leq 0.1$, $b \sim 1/M_\pi$), and understand many other dynamical features. The vanishing of the b -distribution at $x \rightarrow 1$ is due to the definition of the transverse center of momentum and does not imply vanishing of the physical size of the nucleon.

The GPDs, however, contain much more information than the parton densities and elastic form factors alone. They describe the correlation of the quark longitudinal momentum fraction, x , with the transverse momentum transfer to the nucleon, Δ_T . This correlation permits a simple interpretation in terms of an x -dependent spatial distribution of quarks in the nucleon. For $\xi = 0$, the two-dimensional Fourier transform of the GPD with respect to Δ_T describes the spatial distribution of quarks with longitudinal momentum fraction x in the transverse plane. The transverse coordinate, \mathbf{b} , which is Fourier-conjugate to Δ_T , measures the distance of the quarks from the transverse center of momentum of the nucleon. The integral of this spatial distribution over \mathbf{b} gives the total parton density at longitudinal momentum fraction x . This 1+2-dimensional “mixed” momentum- and coordinate representation corresponds to a set of tomographic images of the quark distribution in the nucleon at fixed longitudinal momentum fraction, x , see Fig. 1. It allows for a very visual representation of the nucleon in high-energy scattering processes, which provides a most natural framework for the discussion of dynamical models. At $x \sim 0.3$ one mainly “sees” the core of valence quarks, distributed over transverse distances $b \ll 1$ fm. At $x < 0.1$ the pion cloud becomes visible, extending over transverse distances $b \sim 1/(2m_\pi) \sim 1$ fm. At even smaller momentum fractions, $x \lesssim 0.01$ the partons one observed are mostly the gluons and charge/ flavor singlet quarks produced by gluon radiation. The transverse coordinate representation also naturally lends itself to the discussion of various polarization phenomena. In the case of transverse polarization of the nucleon, the transverse spatial distribution of quarks becomes deformed, which *e.g.* explains the origin of target single-spin asymmetries observed in semi-inclusive DIS (Sivers effect). The construction of such tomographic images of the nucleon is one of the main objectives of theoretical and experimental studies of GPDs.

A fully 3-dimensional space-time image of the nucleon is obtained when taking the Fourier transform of the GPD also with respect to the longitudinal momentum transfer to the nucleon, 2ξ , thus localizing the nucleon also in the longitudinal coordinate [11]. In this case the GPD turns into the Wigner phase space distribution of quarks in the nucleon, describing their simultaneous distribution with respect to the longitudinal momentum x and the conjugate coordinate. A quantum phase space distribution describes the distribution of particles over both coordinate and momentum (or, more generally, pairs of conjugate variables) in a quantum mechanical system and represents the closest analog to a classical phase space density allowed by the uncertainty principle. While quantum phase space distributions are widely used in areas of physics as diverse as condensed matter physics, heavy ion physics, and signal theory, they have never been thoroughly studied for subnuclear systems. The GPDs provide, for the first time, a definition of the phase space density of quarks which is fully consistent with the tenets of quantum field theory and firmly rooted in Quantum Chromodynamics and its renormalization group. Figure 2 illustrates the power of this new representation. Shown is the spatial shape of the nucleon (as defined by contours of equal density) for quarks of several longitudinal momentum fraction, x . These images were obtained with a model GPD which incorporates the present parton density and form factor data. One sees *e.g.* that the effective shape of the nucleon changes with the quark momentum fraction, x . This new 3D representation offers unprecedented possibilities not only for visualizing the nucleon as an extended object in space, but also for understanding the space-time evolution of scattering processes probing the quark and gluon structure of the nucleon.

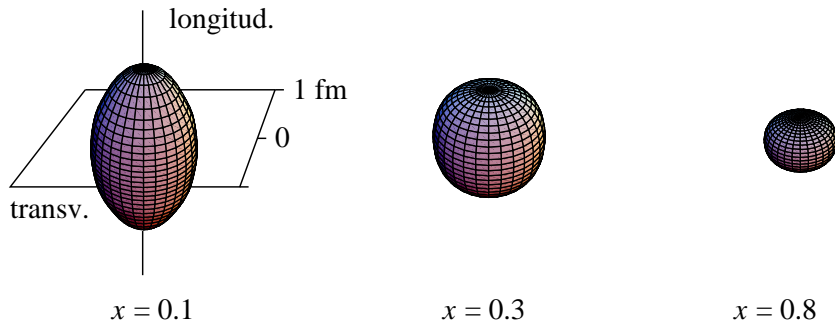


FIG. 2: “3D quark images” of the nucleon, as obtained from a model phase space distribution incorporating phenomenological information about GPD’s [11]. Shown are constant-density surfaces of the spatial distribution of u -quarks, for three values of the momentum fraction, x . In the valence quark region at moderate x (center) the nucleon has spherical shape. At $x \rightarrow 1$ (right) the size shrinks and the shape becomes oblate (disk-like). At small x (left) the quarks spread out in the longitudinal direction, and the shape becomes prolate (cigar-like).

Further motivation for the study of GPDs comes from the fact that certain moments of the GPDs — weighted integrals over the quark momentum fraction, x — are related to fundamental static properties of the nucleon. In particular, the second moment of the GPDs gives the fraction of the nucleon spin carried by the quarks, including their spin and orbital angular momentum [5]. Starting with the historic measurements by the EMC collaboration 20 years ago, polarized DIS experiments aim to determine how the nucleon’s spin is composed from the spins of quark and gluons and their orbital motion. While significant progress has been made in determining the quark spin distributions in the nucleon, little is known about gluon spin, which is to be studied in dedicated experiments at RHIC and COMPASS. Measurements of the GPDs would give access to the quark orbital angular momentum, thus providing information about a crucial other piece of the nucleon “spin puzzle.” The GPDs also provide information about the forces acting on the quarks in the nucleon [12].

Moments of the nucleon GPDs also can be computed in lattice QCD simulations. Lattice QCD methods have made steady progress during the last years and are beginning to yield first results for moments of parton distributions, form factors, and GPDs. While simulations with realistic quark masses and the calculation of quark flavor-singlet and gluonic nucleon properties still pose considerable challenges, significant investments are being made to address these problems. In the long term it certainly will be possible to harness the power of this *ab initio* approach to hadron structure for determining the lowest moments of the GPDs, complementing information obtained from experiment. The anticipated progress in lattice QCD methods is described in a companion White Paper [13].

Experimental information about GPDs comes from measurements of a variety of eN scattering processes probing the quark structure of the nucleon at short distances (see Fig. 3). Fundamental to the analysis of these processes is that the asymptotic freedom of QCD guarantees that the short-distance information specific to the probe can unambiguously be separated from the long-distance information about nucleon structure contained in the GPDs (“factorization theorem”), and that the GPDs represent universal, process-independent characteristics of the nucleon. Important basic information is provided by the data on quark parton densities accumulated in inclusive DIS experiments (both unpolarized and polarized) during the last 30 years, and the data on the nucleon form factors (vector and axial vector) from elastic scattering, see Ref. [14] for a recent review. These data constrain the GPDs in the “diagonal” case, $\xi = 0$ and $\Delta_T = 0$, and its first moments as functions of $t = -\Delta_T^2$ (see Fig. 3b, c). The crucial new information about the correlation of the x, ξ - and Δ_T -dependence, which is needed for constructing the 1+2-dimensional tomographic and 3-dimensional images of the nucleon and for extracting the quark orbital angular momentum, comes from measurements of hard exclusive processes, such as DVCS and meson production (see Fig. 3d, e). In these processes a particle (real photon, meson) is produced in the hard scattering of the electron from a quark, which receives both a longitudinal and a transverse momentum transfer, and they probe the GPDs at $\xi \neq 0$ and $\Delta_T \neq 0$ (the invariant momentum transfer t is a function of ξ and Δ_T^2).

The momentum transfer, Q^2 , in eN scattering defines the spatial resolution of the probe. The description of hard exclusive processes in terms of GPDs applies to the limit of large Q^2 , where the reaction is dominated by the scattering from a single, quasi-free quark (“leading-twist approximation”). At lower Q^2 , effects related to the interaction of quarks during the hard scattering process, or coherent scattering involving more than one quark, become important (“higher-twist effects”). The minimum value of Q^2 required for the GPD description to be applicable in practice

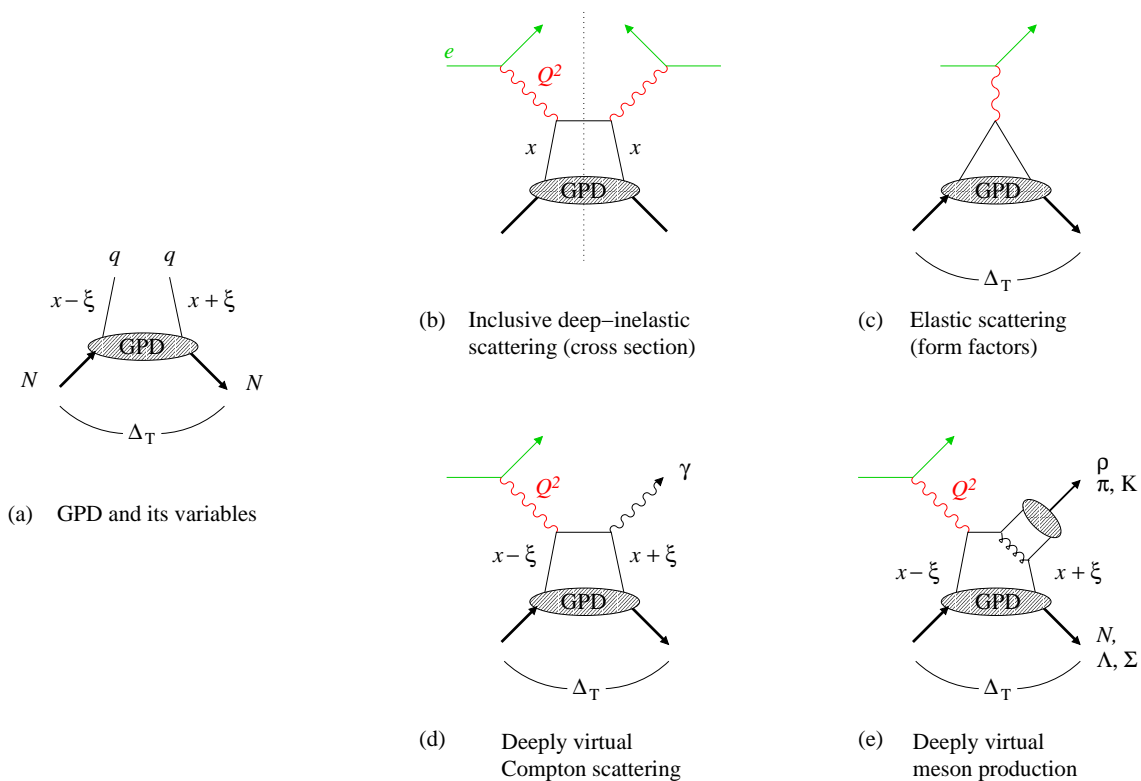


FIG. 3: (a) The GPD describes the amplitude for “taking out” a quark from the nucleon and “putting it back” with different momentum. (b–e) Reactions in eN scattering probing the GPDs. (b) Inclusive DIS probes the GPD’s in the “diagonal” case ($\xi = 0$, $\Delta_T = 0$), where they coincide with the usual parton densities in the nucleon. (c) The elastic form factors of the nucleon constrain the moments (x -integrals) of the GPD’s at non-zero momentum transfer, $\Delta_T^2 = Q^2$. (d, e) DVCS and meson production probe the GPD’s at nonzero longitudinal and transverse momentum transfer, $\xi \neq 0$, $\Delta_T \neq 0$. Different mesons (ρ , π , K) select different spin–flavor components of the GPD’s.

depends on the final state, and can ultimately only be determined experimentally. For DVCS, the experience with inclusive DIS and other two-photon processes (such as $\gamma^* \gamma \rightarrow \pi^0$ measured in e^+e^- annihilation) suggest that the leading-twist approximation should be reliable already at $Q^2 \sim \text{few GeV}^2$, which seems to be consistent with first experimental results on the Q^2 dependence of DVCS observables (see below). Thus, DVCS can be used to extract information about GPDs at the momentum transfers accessible in fixed-target experiments. For meson production, the experience with the pion form factor at high Q^2 and available meson electroproduction data suggest that higher-twist effects result in significant corrections to the GPD description up to momentum transfers of $Q^2 \sim 10 - 20 \text{ GeV}^2$. While these effects can be minimized by studying suitable ratios of observables or polarization asymmetries, or can be corrected for using phenomenological models, it seems likely that the use of meson production data for a quantitative extraction of GPDs requires measurements at significantly higher momentum transfers than in DVCS.

The actual extraction of information about the GPDs from DVCS observables is a complex task, which has been extensively discussed in the recent literature. In the $eN \rightarrow eN\gamma$ cross section, the DVCS amplitude interferes with the known amplitude of the Bethe–Heitler process, in which the final-state photon is emitted from the electron. This fact allows one to separate the imaginary and real parts of the DVCS amplitude by measuring combinations of cross sections and asymmetries with respect to the beam spin (helicity), beam charge (e^+/e^-), and/or target or recoil polarization. The imaginary part of the amplitude probes the GPDs at $x = \xi$, where ξ is related to the usual Bjorken variable by $\xi = x_B/(2 - x_B)$; the real part probes a dispersive integral over the quark momentum fractions. The different nucleon spin components of the GPDs can be separated by measuring target spin asymmetries. Measurements of the t - (Δ_T -) dependence provide the information necessary for transverse nucleon imaging. Study of the flavor decomposition of the quark GPDs (u, d, s) requires measurements with both proton and neutron (*i.e.*, nuclear) targets. Additional information for the spin/flavor separation comes from the meson production data. The DVCS and meson production data are then used to constrain the parameters of theoretical parametrizations of the GPDs, which incorporate the information on the nucleon’s parton densities and form factors gained from previous independent measurements, as

well as knowledge of the general structure of the x, ξ and Δ_T dependence of the GPDs derived from theoretical considerations. Such parametrizations play an essential role in this program, ultimately providing the link between the eN scattering observables and the 1+2-dimensional or 3-dimensional images of the nucleon.

Experimental studies of GPDs through processes such as DVCS and meson production require measurements at center-of-mass energies, W and momentum transfers, Q^2 , in the multi-GeV region, which are accessible only with sufficiently high beam energies. At the same time, since exclusive processes in this kinematics are rare processes (in generic scattering events multiple hadrons are produced), they require high luminosities, as can be achieved in fixed-target experiments with intense beams or in next-generation colliding beam experiments. Finally, the need to guarantee an exclusive final state, and to measure t -distributions of cross sections, places very high demands on the detection equipment, such as good energy resolution in missing mass experiments, or detection of the recoil nucleon. Together, this results in a combination of challenges which has never before been encountered in DIS experiments.

We note that GPDs have interesting applications also beyond the high- Q^2 exclusive processes discussed in this White Paper. At high momentum transfer to the nucleon, $|t| \gg 1 \text{ GeV}^2$, their behavior is closely linked to that of the nucleon elastic form factors — both sample rare small-size configurations in the nucleon wave function. GPDs at high $|t|$ can be probed in real wide-angle Compton scattering, which is expected to proceed effectively via Compton scattering from a single quark in the target, similar to DVCS [15].

III. EXPERIMENTAL RESULTS ON HARD EXCLUSIVE PROCESSES

DVCS and meson production in eN scattering have been studied in several experiments at fixed-target facilities (HERMES at DESY, Jefferson Lab with 6 GeV beam energy) and the HERA collider. These studies have demonstrated the basic feasibility of such measurements, and have provided crucial evidence for the applicability of the GPD-based description of such processes. They are also providing first useful constraints for GPD phenomenology.

DVCS experiments at fixed-target energies aim to extract the interference terms between the DVCS and the Bethe-Heitler (BH) amplitudes in the $eN \rightarrow e'N\gamma$ cross section. The interference terms are experimentally accessible from combinations of measurements of the spin-dependent and independent cross sections and relative asymmetries, as well as from measurements of the beam charge dependence (e^+/e^-) of the cross section. In kinematic regions where the BH amplitude is much larger than the DVCS amplitude, the interference with the BH amplitude acts as a natural “amplifier and filter” for the DVCS amplitude, boosting it to comfortably measurable levels. Measurements of the beam spin asymmetry in $eN \rightarrow e'N\gamma$ were performed by HERMES ($0.02 < x_B < 0.3$) [16] and CLAS at JLab ($0.15 < x_B < 0.55$) [17, 18]. Figure 4 shows the kinematic coverage achieved in the CLAS E01-113 experiment (2005),

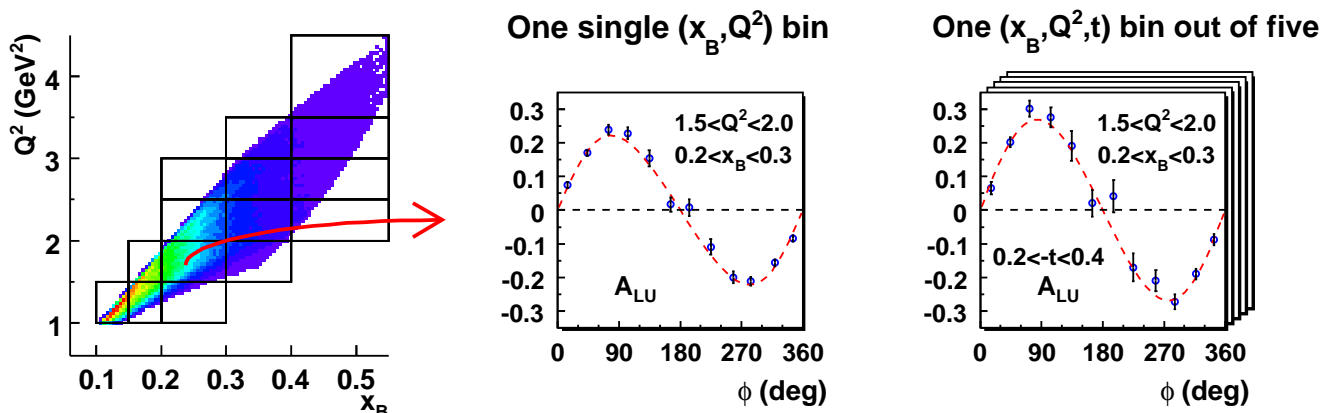


FIG. 4: Measurements of the beam spin asymmetry, A_{LU} , of the $eN \rightarrow e'N\gamma$ cross section in the CLAS E01-113 experiment at JLab with 6 GeV beam energy (preliminary). The plot shows the kinematic coverage in x_B and Q^2 (left), and the azimuthal angle dependence of A_{LU} in a typical (x_B, Q^2) bin, both integrated over t (center) and in of the 5 sub-bins in t (right). The $\sin \phi$ dependence is characteristic of the BH-DVCS interference cross section. The data illustrate the potential for fully differential measurements of the x_B, Q^2 and t -dependence of DVCS observables with this setup.

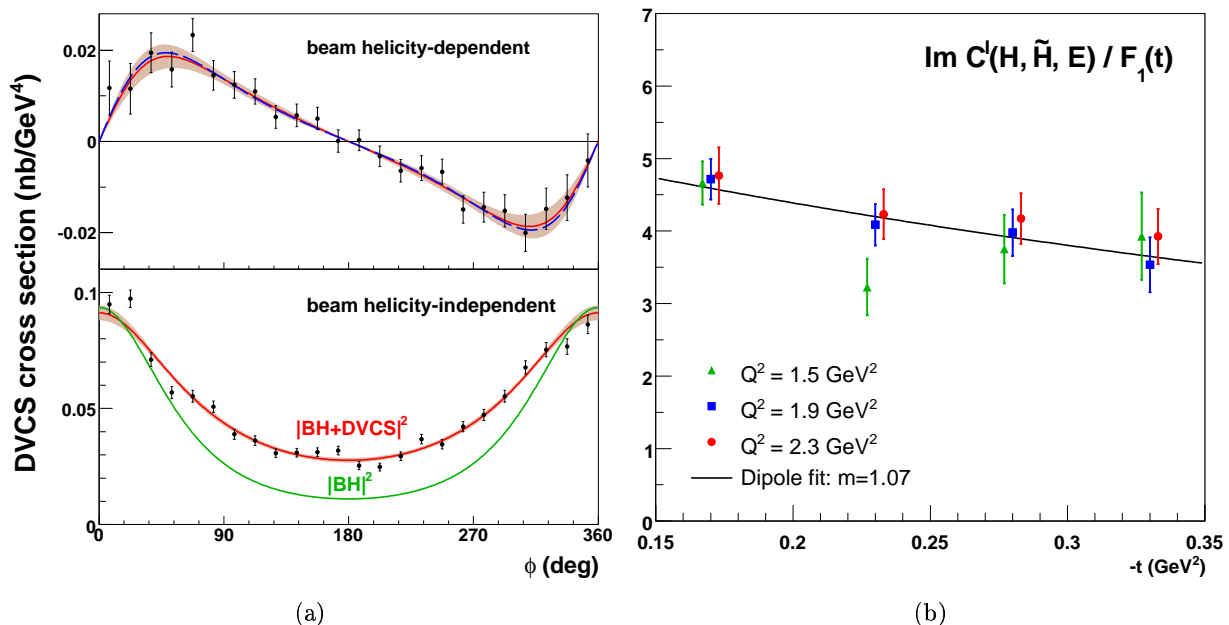


FIG. 5: Measurements of the $eN \rightarrow e'N\gamma$ cross section by the JLab Hall A experiment [20]. (a) The differential cross sections, $d^4\sigma/dQ^2 dx_B dt d\phi$, as a function of the azimuthal angle, ϕ , of the detected real photon, at $Q^2 = 2.3 \text{ GeV}^2$, $|t| = (0.25-0.3) \text{ GeV}^2$, and $x_B = 0.36$. Shown are the beam helicity-dependent (top) and independent (bottom) cross sections. The green curve shows the $|BH|^2$ cross section alone, which is calculable in terms of the known nucleon form factors. The red curve is a fit to the data in which the ϕ -dependence is predicted by theory. The difference between the red and green curve is to be attributed to the BH–DVCS interference as well as the $|DVCS|^2$ terms in the cross section. (b) The coefficient of the beam spin-dependent interference cross section, as a function of t , for different values of Q^2 . The observed Q^2 -independence is consistent with the predictions of the QCD factorization theorem. In the factorization regime, this coefficient is proportional to a linear combination of GPDs. The solid line represents a phenomenological dipole fit to the t -dependence of this linear combination.

and the results for the asymmetry in a typical (x_B, Q^2) bin (integrated over t) as well as in a single (x_B, Q^2, t) bin. This experiment used a new inner calorimeter to detect photons at small scattering angles. The azimuthal angle dependence of the asymmetry clearly exhibits the $\sin \phi$ behavior characteristic of the BH–DVCS interference. This asymmetry can be related to a linear combination of GPDs at $x = \xi$; the experimental results are consistent with the predictions of present GPD models. An important point is that with the CLAS detector data in all (x_B, Q^2, t) bins are taken simultaneously, making it possible to extract information about the GPDs over a wide kinematic range. HERMES also measured the beam charge asymmetry of the cross section [19], which probes a dispersive integral of the GPDs over the quark momentum fractions.

First measurements of absolute cross sections for DVCS were recently performed by the JLab Hall A experiment [20]. A sample of the results is shown in Fig. 5a. The beam spin-dependent $eN \rightarrow e'N\gamma$ cross section (top plot) is directly proportional to a weighted sum of different GPDs at $x = \xi$; the azimuthal angle dependence of the data is consistent with theoretical expectations. The data for the helicity-independent cross section (bottom plot) clearly show the deviation from the calculable BH cross section caused by the DVCS process. An interesting conclusion of this analysis is that for values of ϕ not close to 0° or 360° both the BH–DVCS interference and the $DVCS^2$ term in the cross section seem to contribute substantially to this difference; the separation of the two terms, using their different dependence on the incident beam energy, is the subject of a new proposed experiment. The relative asymmetry (as measured independently by the CLAS experiment, see Fig. 4) is given by the ratio of the top and bottom curves. Figure 5b shows the t - and Q^2 -dependence of the coefficient of the beam-spin dependent interference cross section extracted from the data; this coefficient is directly proportional to a certain linear combination of GPDs with different target spin dependence. Comparison between the results for different Q^2 shows that the data are nicely consistent with the approach to Q^2 -independence (“scaling”) at large Q^2 predicted by QCD factorization. Future measurements with polarized target will be able to isolate the contribution of the different GPDs to this observable. To summarize, the measurements of DVCS cross sections and the beam spin asymmetry carried out at JLab with 6 GeV beam energy support the theoretical expectation of dominance of the single-quark reaction mechanism (leading-twist approximation) for DVCS for momentum transfers $Q^2 \sim \text{few GeV}^2$, essential for the GPD interpretation of these processes. They also demonstrate the feasibility of accurate differential measurements of the t -dependence needed for

reconstructing spatial images of the nucleon from GPDs.

Separation of the different spin/flip components of the GPDs requires measurements with polarized targets, as well as measurements with both proton and neutron (nuclear) targets. First measurements of the longitudinal target spin asymmetry in proton DVCS were reported by CLAS at JLab, which eventually will allow one to separate the contributions from unpolarized and polarized nucleon GPDs. An order-of-magnitude more data are expected from JLab during the next two years, making possible a much more quantitative extraction of GPD parameters. A measurement of the transverse target spin asymmetry was reported by HERMES; this observable is particularly sensitive to the nucleon helicity-flip (Pauli form factor-type) GPD, which enters in the angular momentum sum rule. The JLab Hall A experiment obtained preliminary data on quasi-free neutron DVCS from measurements with a nuclear target; the neutron data are more sensitive to the d -quark GPD than the proton data (proton and neutron GPDs are related by isospin symmetry). Together, the JLab Hall A and HERMES data allow for a first estimation of the quark angular momentum in the proton, *cf.* Fig. 7 and the discussion below. While this method of constraining J_u and J_d is model-dependent, and the present status of GPD parametrizations does not permit us to quote a systematic error for the estimated values of J_u and J_d (the bands in Fig. 7 show the statistical error only), the preliminary results clearly illustrate the potential of DVCS measurements to constrain the quark angular momentum.

Deeply-virtual meson production was studied in a number of experiments at HERMES and JLab. In these processes the GPD description applies to the amplitude with longitudinal (L) polarization of the virtual photon mediating the interaction; the amplitudes with transverse (T) photon polarization generally involve interactions over transverse distances comparable to normal hadronic size which cannot be expressed in terms of the GPDs. In vector meson production (ρ^0, ϕ), the interesting L component of the amplitude can be isolated from the vector meson decay distribution using s -channel helicity conservation — a theoretically motivated approximation, which was found experimentally to work at the $\sim 10\%$ level. In pseudoscalar meson production (π^0, π^\pm, η, K), L and T components of the amplitude need to be separated using the Rosenbluth method, which requires comparing measurements at different beam energies and makes measurements of this channel considerably more demanding than in the vector case. Comparison of the present meson production data with model calculations based on GPDs generally show the presence of substantial higher-twist corrections up to momentum transfers of several GeV^2 . Efforts are being made to calculate these corrections using theoretical models, to an accuracy which would allow one to use these data for the GPD analysis. With these corrections included, meson production can provide valuable information about the spin and flavor decomposition of the GPDs, which is difficult to obtain in DVCS alone.

Extensive measurements of exclusive vector meson production and DVCS have been performed with the HERA collider, at energies ranging from $50 \lesssim W \lesssim 300 \text{ GeV}$ and $10^{-4} \lesssim x_B \lesssim 10^{-2}$. Scattering processes at such high energies exhibit a number of special features — interaction over large longitudinal distances, importance of gluon radiation — which have been the subject of numerous experimental and theoretical studies, and are collectively referred to as “small- x physics.” Exclusive processes in this kinematics probe the GPDs at small values of the parton momentum fractions $x, \xi \sim x_B \ll 1$. In this region the gluon distribution is dominant, and the quarks mostly originate from perturbative QCD radiation by the gluons (“evolution”). A particularly clean probe of the gluon GPD in the nucleon is photon/electroproduction of heavy vector mesons (J/ψ). Measurements of the J/ψ production cross section, including its t -dependence, at HERA [21] have provided useful information about the transverse spatial distribution of gluons in the nucleon and its dependence on x . Corresponding measurements of ρ and ϕ electroproduction at $Q^2 \sim 10 - 20 \text{ GeV}^2$ have confirmed the universality of the gluon GPD implied by QCD factorization. Also measured at HERA was the DVCS cross section [22]; the results are well described by next-to-leading order QCD calculations incorporating QCD evolution of the GPDs. In summary, the HERA results fully confirm the applicability of QCD factorization to exclusive processes at high energies and have demonstrated the potential of such measurements to map the gluon GPD at small x .

IV. GPD MEASUREMENTS WITH JLAB AT 12 GEV

The JLab 12 GeV Upgrade will double the energy of the CEBAF continuous-beam electron accelerator from 6 to 12 GeV, and extend the capabilities of the detection equipment in the experimental halls [1]. This setup will provide a unique combination of high energy, high beam intensity (luminosity), and large-acceptance detectors, which will enable studies of exclusive processes such as DVCS and meson production in the valence quark region. A rich program of measurements aimed at mapping the quark GPDs of the nucleon has been formulated by the user community, and was reviewed by a special Program Advisory Committee in 2006.

Measurements of DVCS and meson production will be carried out with the upgraded CLAS large-acceptance spectrometer in Hall B at luminosities $\sim 10^{35}\text{cm}^{-2}\text{s}^{-1}$, and with the Hall A high-resolution single-arm spectrometer at luminosities $\sim 10^{37}\text{cm}^{-2}\text{s}^{-1}$. DVCS will be accessed both in missing-mass measurements in which the final-state electron and photon are detected, $ep \rightarrow e'\gamma X$ (Hall A, CLAS), and by detecting the electron and recoil proton in events without other charged or neutral tracks, $ep \rightarrow e'pX$ (CLAS). Detection of the photon in the CLAS inner calorimeter, in addition to the recoil proton and scattered electron, provides the exclusivity condition crucial for complete control over different background processes. Each of these methods has its own advantages with regard to background suppression (π^0) and azimuthal angle coverage, and they probe the $ep \rightarrow e'\gamma p$ in regions of different relative magnitude of DVCS and Bethe-Heitler amplitudes. In this way, GPDs can be extracted using both absolute cross section and polarization asymmetry data. The possibility to use both methods in experiments at a single facility represents a crucial advantage of this setup.

To separate the different spin components of the GPDs, measurements of a variety of polarization observables (beam and target spin) will be performed. The beam longitudinal spin asymmetry, A_{LU} , will access mainly the unpolarized Dirac GPD, H . The target longitudinal spin asymmetry, A_{UL} , probes the corresponding polarized GPD, \tilde{H} . The transverse target asymmetry, A_{UT} , is mostly sensitive to the Pauli form factor-type GPD, E , which enters in the angular momentum sum rule. These asymmetry measurements, combined with measurements of the unpolarized cross sections, allow one to probe the GPDs at momentum fractions $x = \xi$, as a function of both x and t . The results can directly be translated into certain transverse spatial images of the nucleon. As an example, Fig. 6 shows the projected results for the Dirac GPD, H , as a function of x and t , and its corresponding transverse spatial representation. Complementary information can be obtained about integrals of the GPDs over the quark momentum fraction. With the help of GPD parametrizations, this information can be used to construct 2-dimensional tomographic images of the nucleon at $\xi = 0$, *cf.* Fig. 1. The flavor components of the GPDs will be separated by performing measurements of DVCS with both proton and nuclear (^2H) targets. Additional information about the flavor structure will come from ratios of meson production cross sections in channels with the same spin/parity quantum numbers, such as η/π^0 and K^*/ρ^+ . These channels will be measured simultaneously with DVCS, not requiring any extra beam time.

The quark angular momentum in the nucleon, J_q , can be estimated if one uses the projected results of measurements of DVCS and meson production observables to constrain GPD parametrizations, which incorporate also information obtained from other measurements (parton densities, form factors). The quark angular momentum is then obtained indirectly, by calculating the second moment of the GPD parametrization. Figure 7a shows the constraints on J_u and J_d from present DVCS data with deuteron (JLab Hall A, sensitive primarily to J_d) and proton target (HERMES, sensitive primarily to J_u) obtained in this way. The preliminary data from JLab Hall A constrain the GPDs only at a single value of x_B ; systematic studies of the x_B dependence of GPD observables over the next

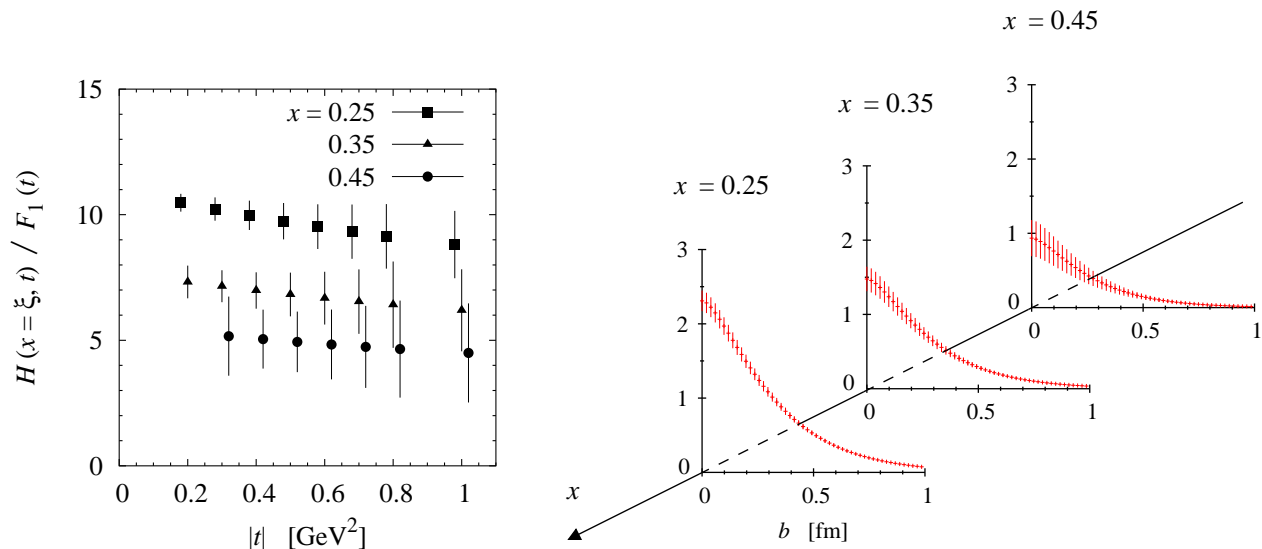


FIG. 6: *Left:* Projected results for the Dirac GPD of the proton, $H(x = \xi, t)$, as a function of x and t , as extracted from the DVCS beam spin asymmetry, A_{LU} , measured with JLab at 12 GeV. Shown is the ratio of the GPD to the the proton's Dirac form, $F_1(t)$. *Right:* Transverse spatial image of the proton obtained by Fourier-transforming the measured GPD [23]. The errors were estimated assuming a dipole-like t -dependence.

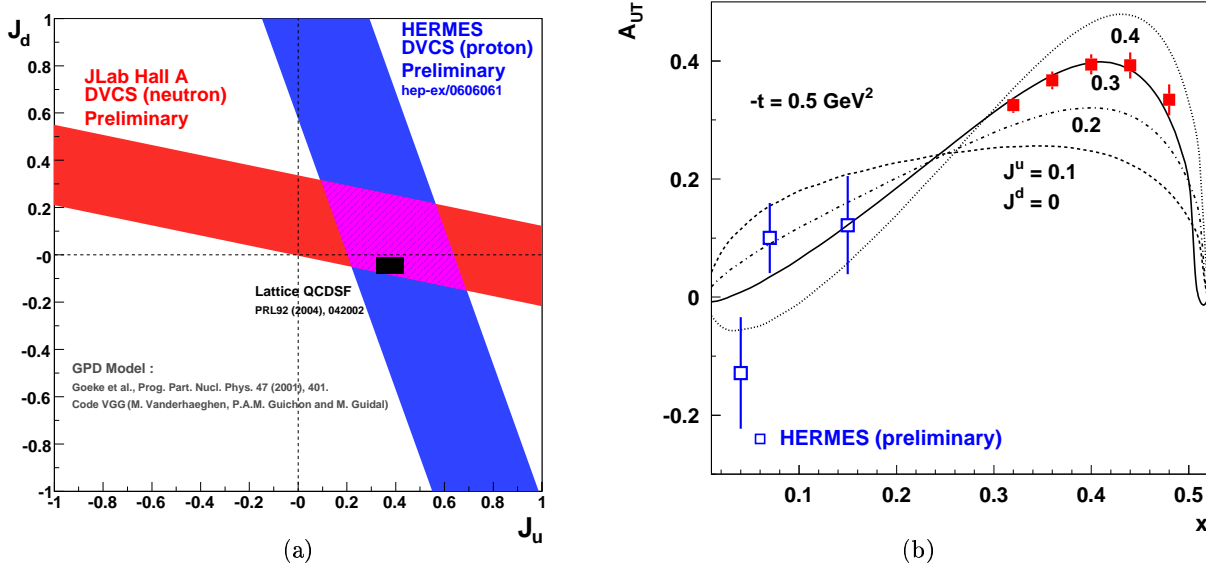


FIG. 7: Projections for experimental determination of the quark angular momentum, J_u and J_d , in hard exclusive electroproduction processes. (a) Constraints on J_u and J_d from present data on quasi-free neutron DVCS with a deuterium target (JLab Hall A, sensitive primarily to J_d), and DVCS with a transversely polarized proton target (HERMES, sensitive primarily to J_u). The data constrain the parameters in a GPD parametrization, which is then used to calculate J_u and J_d . The bands show the statistical error only; no systematic error can presently be quoted for this model-dependent extraction. (b) Sensitivity of the transverse target spin asymmetry, A_{UT} , in hard exclusive ρ^0 electroproduction, $ep \rightarrow e'\rho^0 p$, to J_u , as predicted by a model calculation. Accurate measurements of A_{UT} with JLab 12 GeV (projected data shown in red) will be able to discriminate between these predictions, thus determining J_u .

years will allow us to significantly reduce the uncertainty in this model-dependent extraction and make a realistic error estimate of the values of J_u and J_d . Another useful observable for determining J_u is the transverse target spin asymmetry, A_{UT} , in ρ^0 production, which is particularly sensitive to the Pauli form factor-type GPD, E . Figure 7b shows the sensitivity of the ρ^0 asymmetry to J_u , as predicted by a model calculation of the amplitude based on a GPD parametrization; in this calculation the first moment of the GPD E is constrained by the form factor data, while the second moment is fitted to a given value of J_u . One sees that accurate measurements of the asymmetries will be able to constrain J_u in this way. While not fully model-independent, such methods of extracting J_q will become more and more accurate as GPD parametrizations become more refined as a result of measurements of a variety of other DVCS and meson production observables.

V. GPD MEASUREMENTS WITH A FUTURE ELECTRON-ION COLLIDER

Electron scattering experiments with colliding beams are able to reach substantially higher center-of-mass energies and momentum transfers than fixed-target experiments. The HERA ep collider at DESY, in which 30 GeV electrons collide with 920 GeV protons at a luminosity of $7.5 \times \sim 10^{31} \text{ cm}^{-2} \text{ s}^{-1}$, supported a rich program of studies of QCD at high energies (“small x physics”), where gluon radiation is an essential feature of the dynamics. A polarized high-intensity collider, with tunable energies and the capability to accelerate both proton and nuclear beams (electron-ion collider, or EIC), would be an unique tool for studying both QCD dynamics and nucleon/nuclear structure. The physics program envisaged for such a facility includes study of the gluon spin distribution in the proton, effects of the nuclear medium on the quark and gluon distributions in the proton, the interaction of small-size probes with hadronic matter (color transparency), the approach to the regime of high gluon densities in QCD at high energies, and quark/gluon imaging of the proton through GPD measurements [24].

The development of a high-intensity polarized ep/eA collider presents major technological challenges, which accelerator physicists have begun to address in the last few years. Different designs are being considered, emphasizing

either high energies or high luminosities. The original eRHIC design proposed by BNL [2] would collide a proton or heavy ion beam from the RHIC storage ring (100/250 GeV) with electrons from a 10 GeV storage ring (“ring–ring design”), at an electron–nucleon (eN) luminosity of $10^{33}\text{cm}^{-2}\text{s}^{-1}$. A more ambitious design with a 10 GeV electron linear accelerator (“linac–ring design”) would achieve an eN luminosity of $10^{34}\text{cm}^{-2}\text{s}^{-1}$ this setup would also accommodate multiple interaction regions and allow for an eventual upgrade of the electron energy. In the ELIC design developed by JLab [3], 3–7 GeV electrons in a high–intensity storage ring (fed by the CEBAF accelerator) would collide with protons or light ions from a 30–150 GeV storage ring, achieving eN luminosities from $10^{34}\text{cm}^{-2}\text{s}^{-1}$ (3 on 30 GeV) to $10^{35}\text{cm}^{-2}\text{s}^{-1}$ (7 on 150 GeV); this setup would support four interaction regions. As in fixed–target experiments, measurements of GPDs in hard exclusive processes with an ep/eA collider are much more demanding than traditional inclusive DIS experiments. In addition to requiring substantially higher luminosities because of small cross sections and the need for differential measurements, the detectors and the interaction region have to be designed to permit full reconstruction of the final state.

When assessing the prospects for exclusive measurements at collider energies ($W \gg 10$ GeV) and their physical interpretation, one needs to distinguish between “diffractive” (no exchange of quantum numbers between the target and the produced system) and “non-diffractive” processes (exchange of quantum numbers). In diffractive processes, such as $J/\psi, \rho^0, \phi$ production and DVCS, the cross sections rapidly rise with the collision energy, W . At large Q^2 , they probe the gluon GPD and/or the singlet quark GPD, which in this region is mostly due to gluon radiation. In non-diffractive processes, such as $\pi^\pm, \pi^0, \rho^+, K$ production, the cross sections do not rise significantly or perhaps even decrease with energy. These processes at high Q^2 probe the flavor/charge/spin non-singlet quark GPDs describing the quark structure of the target. They require significantly higher luminosities and are generally much more difficult to measure at high energies than diffractive processes.

Measurements of exclusive reactions in diffractive channels with a high–luminosity ep collider would enable a detailed program of transverse gluon and singlet quark imaging of the nucleon, see Ref. [25] for a review. J/ψ electroproduction is a unique probe of the gluon GPD in the proton, whose t –dependence contains the information about the transverse spatial distribution of gluons. An important simplification arises from the fact that at high energies the gluon GPD is effectively probed in the diagonal case ($\xi \ll 1$) and the momentum transfer to the nucleon is predominantly transverse, $t \approx -\Delta_T^2$, whence the measured t –dependence can be directly translated into tomographic images of the type of Fig. 1. Of particular physical interest is the change of the transverse spatial distribution of gluons with x ; *e.g.*, chiral dynamics predicts that for $x \lesssim 10^{-1}$ the nucleon’s pion cloud should give rise to a distinctive “Yukawa tail” in the transverse spatial distribution of gluons at large b [26]. DVCS and exclusive ρ^0 electroproduction at high Q^2 probe the singlet quark in addition to the gluon GPD. At $x \lesssim 10^{-1}$ and high Q^2 , most of the singlet quarks observed in hard processes are due to gluon radiation (QCD evolution), and the behavior of the singlet quark GPD is closely linked to that of the gluon GPD. The collider would make it possible to measure J/ψ , DVCS, and ρ^0 production under the same conditions, and over a wide range of Q^2 and W . This combination would be a powerful means to test the hard reaction mechanism, study effects of QCD evolution in the GPDs, disentangle singlet quarks and gluon, and take gluonic and singlet quark images of the nucleon of unprecedented detail.

As an example of the precision which could be achieved in such measurements, Fig. 8 shows projected results for DVCS with eRHIC, using both the high–energy (10 on 250 GeV) and low–energy setup (5 on 50 GeV) [2]. The left plots show the total cross section as a function of W , for two different values of Q^2 . They indicate the precision with which the energy dependence of the cross section, assumed here to be of the form $\sigma \propto W^\delta$, could be extracted from the data. The increase of δ with Q^2 reflects the transition from the “soft” to the “hard” reaction mechanism. The right plots show the differential cross section, $d\sigma/dt$, as a function of t , for different x values, and illustrate the precision with which the t –dependence could be mapped for fixed Q^2 and x . Here a t –dependence of the form $d\sigma/dt \propto e^{Bt}$ is assumed. The decrease of B with increasing Q^2 reflects the shrinkage of the effective transverse size of the virtual photon, and provides a crucial test of the approach to the hard reaction mechanism (in the limit $Q^2 \rightarrow \infty$ and fixed x , QCD factorization predicts that the t –dependence becomes independent of Q^2). One sees that with this setup good statistics could be achieved in fully differential measurements in x, Q^2 and t over a wide kinematic range, allowing for numerous detailed studies of the reaction mechanism (Q^2 –scaling behavior, QCD evolution) and extraction of information about the nucleon GPDs (transverse distribution of singlet quarks/gluons). Additional information could come from the comparison of DVCS measurements with electron and positron beams, which are being discussed as an option for eRHIC. In particular, the charge asymmetry of the cross section can separate the real and imaginary parts of the DVCS amplitude, providing valuable insight in the reaction mechanism and useful constraints for the GPD analysis.

Measurements of exclusive meson production in non-diffractive channels with a high–luminosity ep collider would allow for detailed studies of the spin–, flavor– and spatial distributions of quarks in the nucleon at $x \lesssim 0.1$, comple-

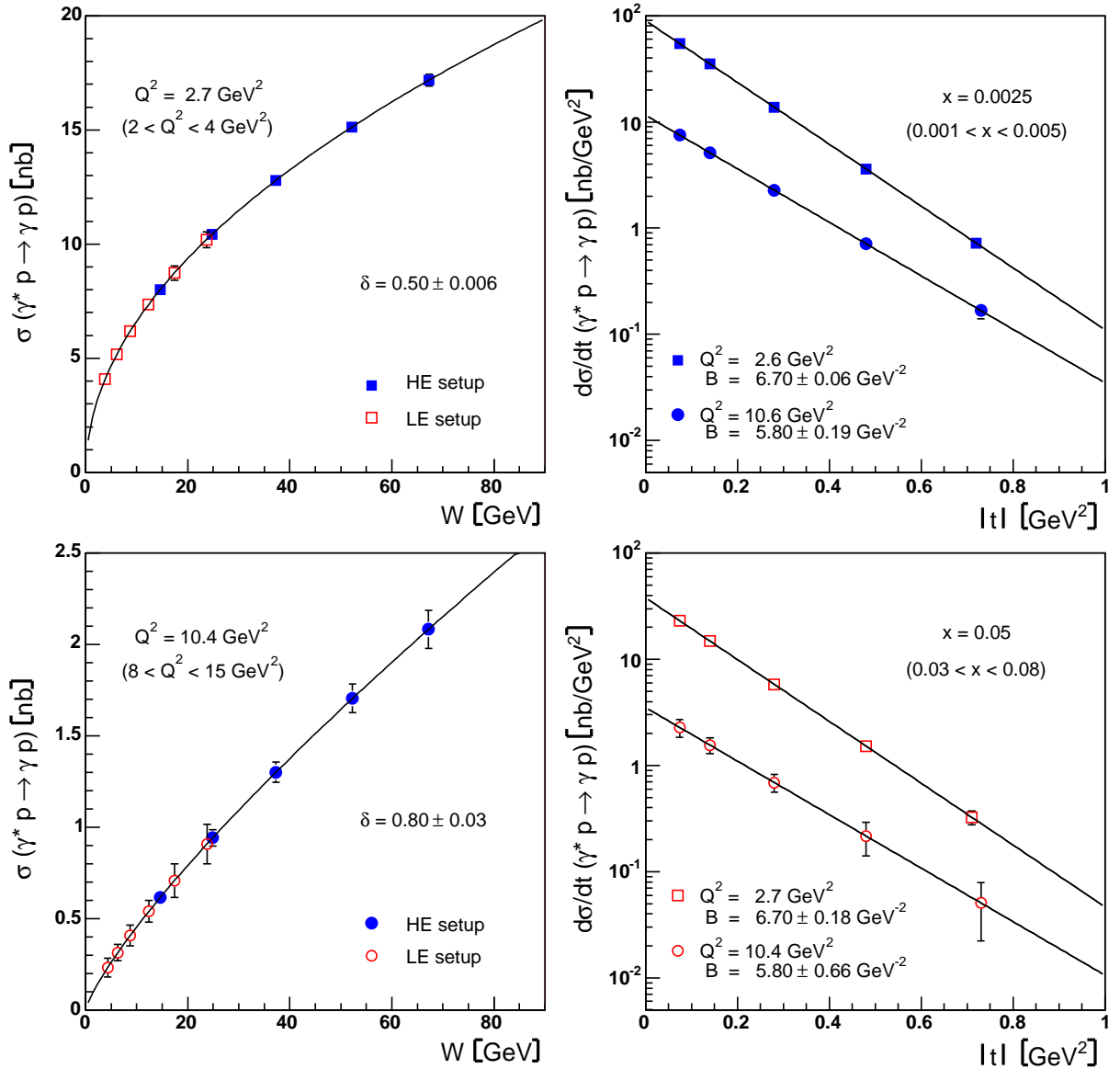


FIG. 8: Projected results of DVCS measurements with an EIC [27]. The simulations refer to the eRHIC ring–ring design, and use both the high–energy (HE, 10 on 250 GeV, blue/filled symbols) and low–energy setup (LE, 5 on 50 GeV, red/open symbols). The assumed integrated luminosities are 530 pb^{-1} (HE) and 180 pb^{-1} (LE), corresponding to two weeks of running at design luminosity with 100% efficiency [2]. The acceptance assumed here is $\sim 90\%$. *Left column:* Total DVCS cross section as function of W , for two Q^2 bins. The simulations assume an energy dependence of the form $\sigma \propto W^\delta$, and the plots show the precision with which the exponent, δ , could be extracted from the data. The increase of δ with Q^2 reflects the transition from the “soft” to the “hard” reaction mechanism. *Right column:* Differential cross section $d\sigma/dt$, as a function of t , for two x bins. A t –dependence of the form $d\sigma/dt \propto e^{Bt}$ is assumed, and the plots show the precision with which the exponent, B , could be extracted from the data. The decrease of B with increasing Q^2 reflects the shrinkage of the effective transverse size of the probe indicative of the hard reaction mechanism. (In this simulation, for simplicity, no x –dependence of B was assumed.)

menting the information from fixed–target experiments in the valence quark region, $x \gtrsim 0.1$. A collider could achieve momentum transfers of the order $Q^2 \sim 10 \text{ GeV}^2$, where higher–twist corrections in the meson production amplitudes are expected to be under theoretical control, and the relation of the GPDs to the experimental observables is more straightforward. Much interesting information can already be gained by comparing observables for different mesonic channels, without detailed modeling of the GPDs. For example, comparison of π^0 and η provides model–independent information about the ratio of the quark spin distributions Δu and Δd and their spatial distributions; it also tests the effect of the $U(1)$ axial anomaly on the meson wave functions [28]. Comparison between π^+ and K^+ production, as well as between ρ^+ and K^{*+} , allows one to study $SU(3)$ flavor symmetry breaking in the nucleon’s quark distributions

in different spin/parity channels and in the meson wave functions. More information about the spatial distribution of quarks can be obtained from the GPD analysis of the absolute cross sections (σ_L) in these channels. Separation of the various response functions (L, T , etc.) would provide a crucial test of the dominance of the single-quark reaction mechanism across the Q^2 and W landscape. Because of the much smaller cross sections in non-diffractive than in diffractive meson production channels at large W , such measurements would require significantly higher luminosity and/or running time for comparable statistics.

Another interesting class of processes which could be studied with a properly designed ep collider are exclusive reactions with $N \rightarrow N^*$ transitions [29]. These processes probe the “transition GPDs” — the probability amplitude for the nucleon to undergo a transition to an excited state when “taking out” a quark and “putting it back” with different momentum. In these reactions the hard scattering process can be regarded as an operator inducing an $N \rightarrow N^*$ transition. An interesting aspect is that in this way one can probe transition quantum numbers which are not accessible with standard electroweak currents (*e.g.* spin > 1). This opens up many new possibilities for studies of resonance structure, which theorists have just started to explore. Equally interesting are hard processes with transition to a non-resonant low-mass πN state; the $N \rightarrow \pi N$ transition GPDs are constrained by chiral dynamics (soft-pion theorems) [30] and can be studied using methods of effective chiral field theory. Such measurements require specially designed detectors, capable of detecting the decay products of the recoiling nucleon resonance.

An electron-ion (eA) collider would also offer numerous opportunities for measurements of exclusive processes with nuclear targets. QCD factorization for meson production at high Q^2 is intimately related to the notion of color transparency — the fact that small-size quark-gluon configurations interact weakly with hadronic matter [25]. Measurements of such processes with nuclear targets across a wide range of W and Q^2 , in which the longitudinal extension of the interaction region in the nucleus rest frame (coherence length), $1/(2m_N x_B)$, is put in relation to the nuclear radius, would allow one to perform detailed tests of color transparency, greatly enhancing our understanding of QCD dynamics at small x . They would also serve as novel tools for exploring nuclear structure in terms of the quark and gluon degrees of freedom of QCD. Coherent DVCS from nuclei would in principle offer a chance to measure nuclear radii with probes other than elastic electron scattering, mapping *e.g.* the mass rather than the electric charge and current distributions in the nucleus. Such measurements with nuclear targets place very high demands on the detectors (detection/vetoing of target fragments) and on the accelerator design (intrinsic transverse momentum spread in the beam), and are presently the subject of exploratory studies.

VI. PERSPECTIVES OF HARD EXCLUSIVE PROCESSES AND GPDs

The concept of GPDs and the idea of spatial imaging of the nucleon have revolutionized nucleon structure studies in QCD. The JLab 12 GeV Upgrade will allow scientists to map the nucleon GPDs in the valence quark region at large x , exploring its quark structure in unprecedented detail. An EIC, as a logical next step, would map the gluon and quark GPDs at small x , relating GPDs to the rich program of studies of QCD dynamics at high energies. To conclude our outlook, we would like to briefly comment on how the program of exploring nucleon structure in terms of GPDs relates to current developments in other areas of nuclear and hadronic physics.

The exploration of the quark structure of the nucleon through GPDs at large x will make full use of the anticipated progress in lattice QCD [13]. Lattice simulations will be able to provide increasingly accurate estimates of certain lowest moments of the quark GPDs, *e.g.* the quark angular momentum, or the nucleon form factors of the QCD energy-momentum tensor, which can be used to fix parameters in general GPD parametrizations. An important point is that, for the foreseeable future, lattice methods will be able to estimate flavor-nonsinglet quark GPDs much more accurately than singlet quark or gluon GPDs; this should be considered when combining experimental data and lattice results in GPD studies.

The gluon GPD at small x is an important ingredient in modeling $pp/\bar{p}p$ collisions at high energies (LHC, Tevatron, RHIC). Knowing the transverse spatial distribution of gluons from measurements of hard exclusive processes in ep scattering, one can describe the “transverse geometry” in pp collisions with hard QCD processes and control many of their fascinating properties. In particular, this information is essential for modeling the approach to the new regime of high gluon densities (saturation, unitarity limit) in high-energy $pp/pA/eA$ collisions. It is even possible to probe certain aspects of the gluon GPD in high-energy pp collisions, *e.g.*, by measurements of the transverse momentum distribution in exclusive hard diffractive pp scattering in future experiments at the LHC [31]. More generally, the spatial view of the partonic structure of the nucleon enabled by the GPDs naturally leads to a convergence of methods

used to describe high-energy lepton/photon-induced and hadron-induced processes.

QCD as a field theory of strong interactions can be solved analytically only at short distance scales, where the effective coupling is weak and methods of perturbation theory and the renormalization group can be applied. The search for an effective theory with simple properties which could replace QCD in the non-perturbative domain remains perhaps the foremost problem of strong interaction physics. Recently, approaches based on the idea of the duality of gauge and string theories (“AdS/CFT correspondence”) have produced very encouraging results. Dynamical models based on these ideas can explain *e.g.* the gross properties of the meson spectrum (Regge trajectories), as well as the observed scaling behavior of high-energy amplitudes (counting rules). The theory of hard exclusive scattering processes, which probe the quark-hadron interface at the amplitude rather than the cross section level, is becoming an important testing ground for these approaches [32, 33].

-
- [1] Conceptual Design Report (CDR) for The Science and Experimental Equipment for The 12 GeV Upgrade of CEBAF (Prepared for the DOE Science Review, April 6–8, 2005), Editors J. Arrington *et al.*, Jefferson Lab (2005); available at: www.jlab.org/div_dept/physics_division/GeV/doe_review/CDR_for_Science_Review.pdf
- [2] eRHIC Zeroth-Order Design Report, Editors M. Farkhondeh and V. Ptitsyn, BNL; available at http://www.bnl.gov/cad/eRhic/eRHIC_ZDR.asp
- [3] Zeroth-Order Design Report on the Electron-Light Ion Collider at CEBAF; Editor L. Merminga (2007).
- [4] D. Mueller *et al.*, Fortsch. Phys. **42**, 101 (1994).
- [5] X. D. Ji, Phys. Rev. D **55**, 7114 (1997).
- [6] A. V. Radyushkin, Phys. Lett. B **385**, 333 (1996); Phys. Rev. D **56**, 5524 (1997)
- [7] K. Goeke, M. V. Polyakov and M. Vanderhaeghen, Prog. Part. Nucl. Phys. **47**, 401 (2001).
- [8] M. Diehl, Phys. Rept. **388**, 41 (2003).
- [9] A. V. Belitsky and A. V. Radyushkin, Phys. Rept. **418**, 1 (2005).
- [10] M. Burkardt, Int. J. Mod. Phys. A **18**, 173 (2003).
- [11] A. V. Belitsky, X. D. Ji and F. Yuan, Phys. Rev. D **69**, 074014 (2004)
- [12] M. V. Polyakov, Phys. Lett. B **555**, 57 (2003).
- [13] C. Morningstar *et al.*, White Paper contributed to APS DNP Joint Town Meetings on Quantum Chromodynamics, Rutgers University, Jan. 12–14, 2007, available at: http://www.physics.rutgers.edu/np/lattice_hadron_whitepaper.pdf
- [14] C. F. Perdrisat, V. Punjabi and M. Vanderhaeghen, arXiv:hep-ph/0612014.
- [15] A. V. Radyushkin, Phys. Rev. D **58**, 114008 (1998); M. Diehl *et al.*, Eur. Phys. J. C **8**, 409 (1999).
- [16] A. Airapetian *et al.* [HERMES Collaboration], Phys. Rev. Lett. **87**, 182001 (2001).
- [17] S. Stepanyan *et al.* [CLAS Collaboration], Phys. Rev. Lett. **87**, 182002 (2001).
- [18] S. Chen *et al.* [CLAS Collaboration], Phys. Rev. Lett. **97**, 072002 (2006).
- [19] F. Ellinghaus [HERMES Collaboration], Nucl. Phys. A **711**, 171 (2002); A. Airapetian *et al.* [HERMES Collaboration], arXiv:hep-ex/0605108.
- [20] C. Munoz Camacho *et al.* [Jefferson Lab Hall A Collaboration], Phys. Rev. Lett. **97**, 262002 (2006); arXiv:nucl-ex/0609015.
- [21] A. Aktas *et al.* [H1 Collaboration], Eur. Phys. J. C **46**, 585 (2006); S. Chekanov *et al.* [ZEUS Collaboration], Nucl. Phys. B **695**, 3 (2004).
- [22] C. Adloff *et al.* [H1 Collaboration], Phys. Lett. B **517**, 47 (2001); A. Aktas *et al.* [H1 Collaboration], Eur. Phys. J. C **44**, 1 (2005). S. Chekanov *et al.* [ZEUS Collaboration], Phys. Lett. B **573**, 46 (2003).
- [23] M. Diehl, Eur. Phys. J. C **25**, 223 (2002).
- [24] The Electron Ion Collider, White Paper, BNL Report BNL-68933, February 2002.
- [25] L. Frankfurt, M. Strikman and C. Weiss, Ann. Rev. Nucl. Part. Sci. **55**, 403 (2005)
- [26] M. Strikman and C. Weiss, Phys. Rev. D **69**, 054012 (2004).
- [27] A. Sandacz, presented at Joint INT/JLab/BNL Workshop “Hard exclusive processes with JLab 12 GeV and a future EIC,” University of Maryland, Oct. 29–30, 2006.
- [28] M. I. Eides, L. L. Frankfurt and M. I. Strikman, Phys. Rev. D **59**, 114025 (1999).
- [29] L. L. Frankfurt, M. V. Polyakov, M. Strikman and M. Vanderhaeghen, Phys. Rev. Lett. **84**, 2589 (2000).
- [30] M. V. Polyakov and S. Stratmann, arXiv:hep-ph/0609045; V. M. Braun *et al.*, Phys. Rev. D **75**, 014021 (2007).
- [31] L. Frankfurt, C. E. Hyde, M. Strikman and C. Weiss, Phys. Rev. D **75**, 054009 (2007).
- [32] S. J. Brodsky and G. F. de Teramond, Phys. Lett. B **582**, 211 (2004).
- [33] A. V. Radyushkin, Phys. Lett. B **642**, 459 (2006). H. R. Grigoryan and A. V. Radyushkin, arXiv:hep-ph/0703069.